Silicon (2019) 11:2421–2428
DOI 10.1007/s12633-016-9519-4

ORIGINAL PAPER

Physical and Structural Properties of Lithium Borate Glasses Containing MoO_3

KH. S. Shaaban[1] · **S. M. Abo-Naf**[2] · **M. E. M. Hassouna**[3]

Received: 24 August 2016 / Accepted: 27 October 2016 / Published online: 12 May 2017

Abstract Lithium borate glasses Li_2O–MoO_3–Al_2O_3–B_2O_3 have been prepared and analyzed using some physical parameters such as the density, the molar volume, IR and UV spectroscopies along with an ultrasonic technique. The values of the optical band gap E_g for indirect transition, and refractive index have been determined for different compositions of the amorphous glass and correlated with the results of FTIR, ultrasonic wave velocities and elastic moduli.

Keywords Lithium borate glasses: molybdenum · IR · Thermal analysis · Density · Ultrasonic · UV- spectroscopy

1 Introduction

Due to the importance of the lithium borate glasses in science and technology, the characterization of these glasses modified with different oxides is strongly needed, given their important advantages as solid electrolytes in storage batteries. The physical properties of borate based glasses can often be altered by the addition of a network modifier such as an alkali and alkaline earth oxide to the basic constituent (network former B_2O_3). It was observed that the properties of borate glasses modified with alkali oxide showed a non-linear optical behavior when the alkali oxide was gradually increased [1]. Lithium borate glass has a wide range of application; it can be used for detecting penetration of radiation which is applied in homeland security and non-proliferation and also for optical lenses because it has high refractive index [2].

The molybdenum in Li_2O-B_2O_3 glasses has at least two stable valence states; Mo^{5+} and Mo^{6+} depending upon their concentration and chemical composition of the host network [4]. Studies on this type of glasses concluded that the ratio of different states of molybdenum control the polarizability of the oxygen surrounding the paramagnetic ions, the concentration of non-bridging oxygens (NBO) and the coordination number [1–5].

IR spectroscopy is a very sensitive and one of the most used spectroscopic methods in the investigation of the local order characterizing vitreous materials like glasses. The borate glasses are very often investigated by many different methods because they are relatively easy to obtain, and because a large variety of structural units over a wide range of modifier concentration appears in their structure [6].

The aim of the present work is to investigate the influence of Li_2O on the structure and physical properties of the molybdenum borate glasses by means IR, ultrasonics, UV spectroscopy, density and differential thermal analysis (DTA).

2 Experimental Procedures

In order to prepare glass samples having the nominated chemical compositions as listed in Table 1, appropriate amounts of analytically pure grade chemicals (Aldrich 99.8%) of H_3BO_4, Li_2CO_3, Al_2O_3 and MoO_3 were thoroughly mixed in an agate mortar and melted in a ceramic

✉ KH. S. Shaaban
khamies1078@yahoo.com

[1] Faculty of Science, El-Azhar University, Assiut 71524, Egypt

[2] Glass Research Department, National Research Centre, El-Behoos Str., Dokki, 12622 Cairo, Egypt

[3] Chemistry Department, Faculty of Science, Beni-Suef, Egypt

Table 1 Nominal chemical composition (mol%)

Glass	B_2O_3	Li_2O	Al_2O_3	MoO_3	ρ	V_m	VL	VT	K	Y
no.	mol%				(g/cm^3)	(cm^3/mol)	(m s^{-1})		(GPa)	
G1	73.55	16.55	1.84	8.06	2.51	3641.6	5860	3516	44.82	79.47
G2	69.13	21.20	1.84	7.83	2.53	3576.92	5819	3491	44.56	78.97
G3	58.43	32.46	1.86	7.26	2.63	3219.34	5793	3475	45.92	81.34
G4	53.93	37.19	1.86	7.02	2.65	3156.02	5766	3459	45.83	81.21
G5	44.86	46.73	1.87	6.54	2.68	2993.37	5730	3438	45.76	81.12

crucible in an electric furnace at 950 °C for about 1 h until a bubble-free liquid was formed. The melts were rotated each 20 min in order to achieve homogeneity. The melt was cast in a stainless steel mold and subsequently annealed at 350 °C, in a muffle furnace. After 30 min, the muffle was switched off and the furnace temperature was left to decrease to the room temperature. The amorphous state of the glasses was checked using X-ray diffraction.

The infrared absorption spectra of the glasses in the wave number range of 400–2000 cm^{-1} with a resolution of 4 cm^{-1} were measured at room temperature by an infrared spectrophotometer type JASCO, FT/IR – 430 (Japan), using the KBr pellet technique, in the ratio 1:100 mg (powder:KBr, respectively), The infrared spectra were corrected for the dark current noises by smoothing ratio 5, and normalized to eliminate the concentration effect. 2 mg of powdered glass was mixed with 200 mg of KBr and the mixture was subjected to a load of 5 tons/ cm^2 to produce a clear homogeneous disk [7, 8]. The FTIR spectra were measured immediately after preparing the disks. The deconvolution procedure is typically repeated iteratively for best results. At iteration, the line shape is adjusted in an attempt to provide narrower bands without excessive distortion.

DTA is the technique measuring the heat effects associated with the physical changes that take place in the glass sample on heating at a constant rate. A micro-DTA apparatus of Shimadzu was used for the DTA investigation. The (15 mg) powdered glass samples were placed in a platinum crucible and examined up to 700 °C in nitrogen medium with a heating rate of 10 °C/min.

Glass densities were measured using Archimedes method. Density was calculated according to the formula;

$$\rho = \rho_0 \frac{(W - W_t)}{(W - W_t) - (W_l - W_{lt})}$$

where ρ is the density of the glass, ρ_0 is the density of the liquid (toluene), W and W_l are the weights of the glass samples in air and toluene respectively, W_t and W_{lt} are weights of the suspended Teflon wire (0.01 mm diameter) in air and in toluene respectively.

The ultrasonic velocities, longitudinal (V_L) and shear (V_T), were obtained using the pulse-echo method. The two velocities besides the density were utilized to determine two independent second-order elastic constants, L and G. For pure longitudinal waves $L = \rho v_L^2$, and for pure transverse waves $G = \rho v_T^2$. The elastic bulk modulus (K) and Young's modulus (Y) can be determined.

The transmittance T (λ) and reflectance R (λ) at normal incidence for the prepared glasses were recorded at room temperature in the wavelength range 300–1100 nm using a computerized double beam spectrophotometer, type JASCO V- 670.

3 Results and Dissociations

3.1 IR Spectroscopy

In the studied glasses, the IR features as shown in Fig. 1, located below 600 cm^{-1} are attributed either to cationic vibrations in the network [9] or to various modes of Al-O-Al vibrations overlapped with the vibrations of the Mo-O bonds in distorted MoO_6. As discussed previously, in certain

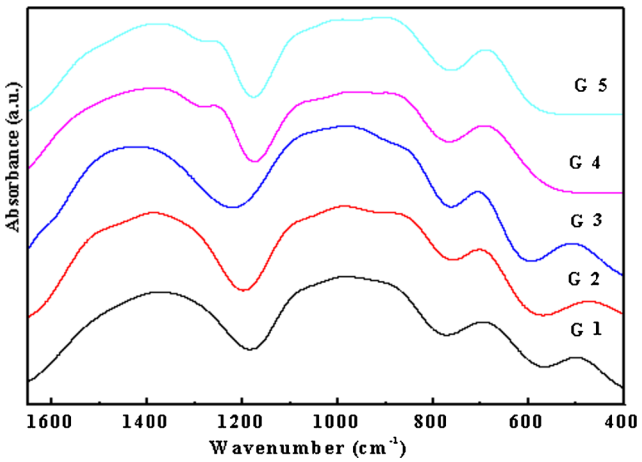

Fig. 1 Infrared spectra of the investigated glasses

cases, Al_2O_3 can form AlO_4 tetrahedra that behave as network former units in the glass structure. An evidence for formation of such units is the appearance of an absorption peak around 650–800 cm^{-1} in the infrared spectra [10]. This peak is not observed in Fig. 1, and so, the formation of condensed or isolated AlO_4 units in the studied glasses can be excluded. Moreover, bending vibrations of B–O–B in BO_3 triangles were attributed to the vibrations of the absorption peak around 690 cm^{-1}. It was reported that glasses containing sufficiently high concentrations of MoO_3 have absorption bands in the range of 750 to 900 cm^{-1} [11]. These bands are attributed to stretching vibrations of Mo-O in MoO_4 units [11]. These units have a former role. In the studied glasses, the absorption bands are located at 750 to 900 cm^{-1}, so that Mo^{3+} ions are supposed to be coordinated with six and four oxygen atoms as MoO_6 or MoO_4. The vibrational bands around 900–1200 cm^{-1} are attributed to the stretching vibration of BO_4 units in various structural groups, see Tables 2 and 3.

On the other hand, the strongest absorption bands of the borate structural units located in the range of 1200–1600 cm^{-1} are attributed to B–O symmetric stretching of $[BO_3]$ groups, the absorption bands that lie in the 900–1119 cm^{-1} range are assigned to B–O stretching of $[BO_4]$ units and the absorption bands in the 675–696 cm^{-1} region are attributed to the bond-bending vibration of B–O–B units [12]. The increase in the Li_2O content in the glass system causes a shift of the absorption band at 900–1119 cm^{-1} to higher wavenumbers which can be attributed to the formation of BO_4 structural units with higher stretching force constant at the expense of BO_3 structural units which have lower stretching force constant [12]. These spectral features lead to an increase in the number of the linked boron based polyhedra, and thus the polymerization degree of the B–O band increases, as the increase of Li_2O content will be accompanied by an increase in the degree of covalent bonding in the glass [13], see Tables 2 and 3.

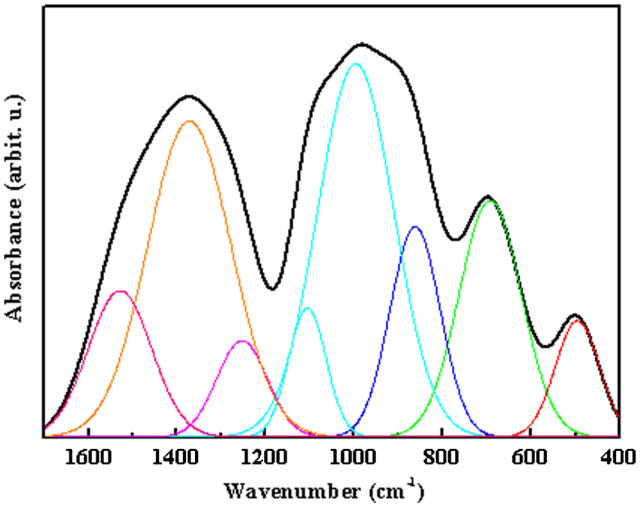

Fig. 2 Curve-fitting of IR spectra of the glasses number G1

Tables 2 and 3 summarize the characteristic parameters of IR absorption bands along with their assignment. Figures 2, 3, 4, 5 and 6 depict the curve fitting of the IR spectra of the studied glasses by using peak fitting on origin 6. There is a good agreement between the glasses and those from the literature [14, 15].

3.2 Density and Mechanical Characterizations

As shown in Fig. 7, the density increases markedly with increasing Li_2O content at the expense of B_2O_3, which has greater molecular mass. The density can be related to the type of structural units that form when Li_2O is incorporated into the glass structure. Li_2O converts symmetric BO_3 triangles into BO_4 tetrahedra or converts the latter into asymmetric BO_3 triangles. Both the BO_4 tetrahedra and asymmetric BO_3 triangles are considerably denser than the symmetric BO_3 triangles [16]. A compensation of the negative charge on the BO_4 tetrahedra would come from positively charged structural defects in the MoO_3 sub

Table 2 Deconvolution parameter of the infrared spectra of studied glasses (C) is the component band center and (A) is the relative area (%) of the component band and (I) is the width component band

G1	C	495	693	862	996	1106	1253	–	1372	1529
	A	4.8	14.2	10.1	27.4	4.6	4.7	–	25.4	8.8
G2	C	–	690	853	982	1102	1238	1316	1441	1576
	A	–	12.8	9.8	24.3	6.4	4.8	10.9	23.7	7.3
G3	C	474	694	843	997	1116	1274	–	1384	1527
	A	3.2	9.9	14.1	27.6	5.9	4.7	–	25.1	9.6
G4	C	508	696	837	973	1110	–	–	1384	1532
	A	4.4	6.1	2.1	46	4.3	–	–	27.7	9.2
G5	C	–	685	882	1030	1109	1240	1312	1422	1545
	A	–	10.7	25.6	17	4.4	4.8	9.7	21.9	5.9

Table 3 Observed IR bands and their assignments

Wavenumber (cm^{-1})	Assignment
400–600	Bending vibrations of Al-O-Al. This band may be overlapped with the vibrations of the Mo-O bonds in distorted MoO_4
600–800	Bending vibration of B–O–B in BO_3 triangles
800–1200	Stretching vibration of BO_4 units in various structural groups. These bands are overlapped with a band attributed to stretching vibrations of Mo–O–Mo of [MoO_4]
1200–1600	B–O stretching vibrations of trigonal BO_3 units only.
1700–2000	H_2O molecules or OH groups

network or from one of the positive charges of Li^+ or Mo^{3+} cations for each BO_4 tetrahedron. As deduced from the analysis of infrared spectra, formation of bridging oxygen ions in the borate matrix is expected due to the former role of MoO_3. The increase in density indicates that the volumes of BO_4 units linked to Li^+ or Mo^{3+} cations have considerably smaller volume than those compensated with positive sites in the borate network. Formation of BO_4 units linked to Li^+ or Mo^{3+} cations would then cause a contraction in the molar volume, as shown in Fig. 7.

The longitudinal (V_L) and shear ultrasonic (V_T) velocities of the glass system with different mol% of Li_2O content are depicted in Fig. 8. It was found that both velocities (V_L and V_T) were decreased as the Li_2O content increased and the values of (V_L) are higher than (V_T). The decrease of the ultrasonic velocity of the studied glasses can be attributed to the lower bond strength of Li–O (341 k J.mol^{-1}) than that of B–O (392 k J.mol^{-1}) [17–20].

Young's modulus is defined as the ratio of the linear stress to the linear strain, [21] i.e., Young's modulus can be related to the bond strength of the materials. The bulk modulus (K) is defined as the change in volume when a force is acted upon it in all directions. In this work, the elastic moduli behave in the same manner as observed for density as shown in Fig. 9 i.e., it depends on the molecular mass of the structural units and on the compactness of the structure as observed from the decrease of the molar volume.

3.3 Thermal Analysis

DTA investigations of the studied glasses were carried out to determine the characteristic temperatures (T_g, T_c, T_p and T_m). T_g is the glass transition temperature characterized by a small endothermic peak, T_c the is onset of the crystallization peak, T_p is the temperature of the peak of crystallization and Tm is the melting temperature. There is no simple technique of formulating the correlation between the ideal composition and the stability of glasses. Different quantitative methods have been suggested to evaluate the level of stability of glassy alloys. Most, for example the method of Dietzel [22], are based on characteristic temperatures (T_g,

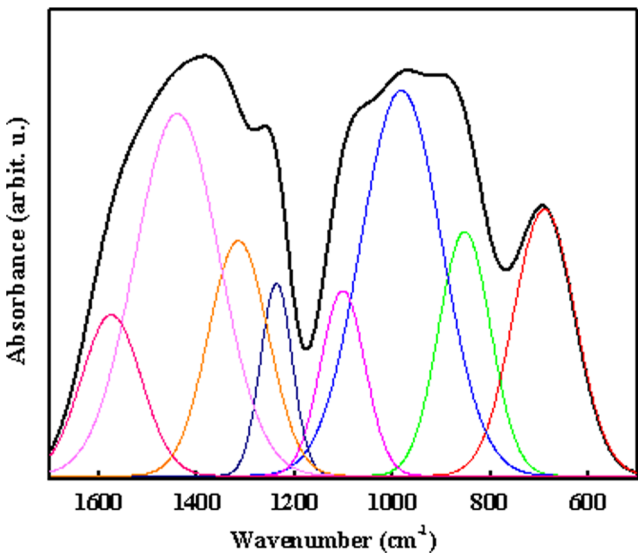

Fig. 3 Curve-fitting of IR spectra of the glasses number G2

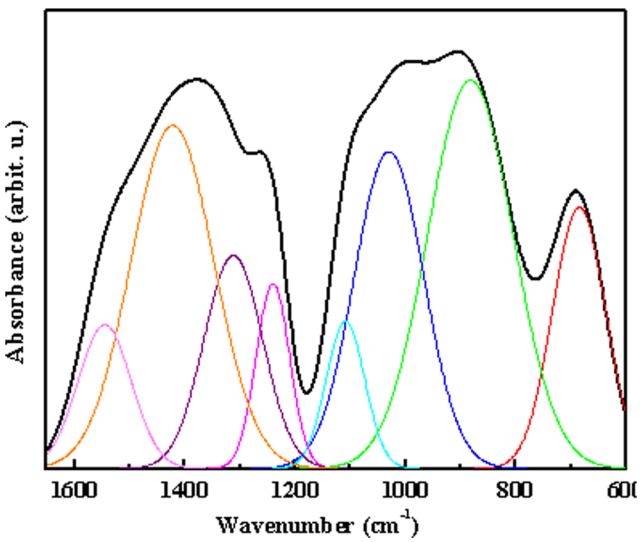

Fig. 4 Curve-fitting of IR spectra of the glasses number G3

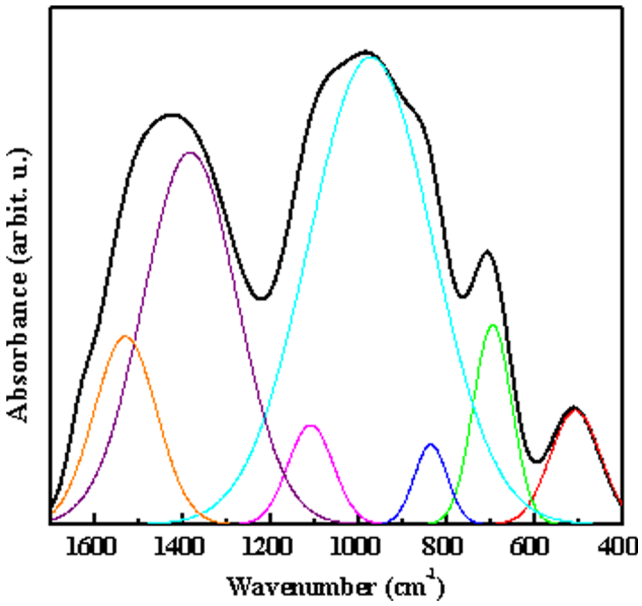

Fig. 5 Curve-fitting of IR spectra of the glasses number G4

T_c and T_p). Dietzel [21] introduced the first glass criterion, $\Delta T = (T_c - T_g)$, which is an important parameter to evaluate glass-forming ability. Saad and Poulain [23] obtained two other criteria: $Hg = \Delta T/T_g$ and $S = (T_p - T_c)\Delta T/T_g$ [23].

The DTA curves of the studied glasses are shown in Fig. 10. In this figure a single endothermic peak is related to the glass transition temperature (T_g), followed by the onset crystallization temperature (T_c), while the exothermic peak is attributed to the full crystallization temperature (T_p). The single peak of (T_g) reveals the good homogeneity of the as-prepared glasses [24]. The decrease in T_g values with increasing Li_2O content may be attributed to

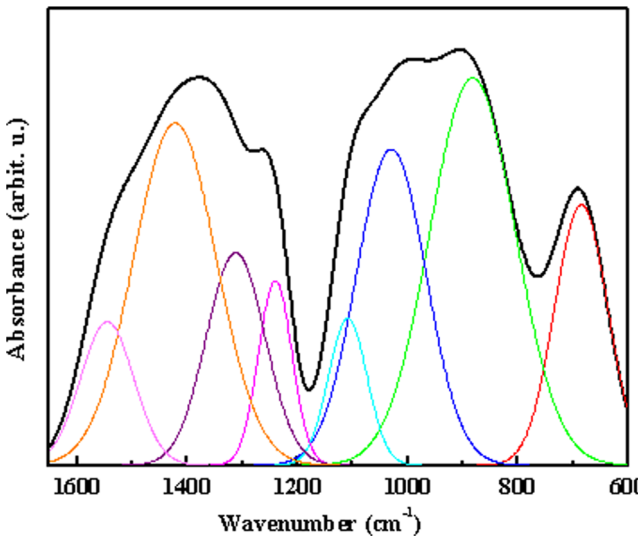

Fig. 6 Curve-fitting of IR spectra of the glasses number G5

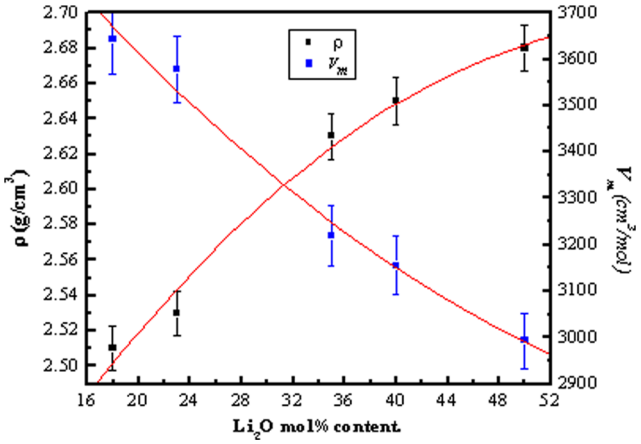

Fig. 7 Density and molar volume of the investigated glasses

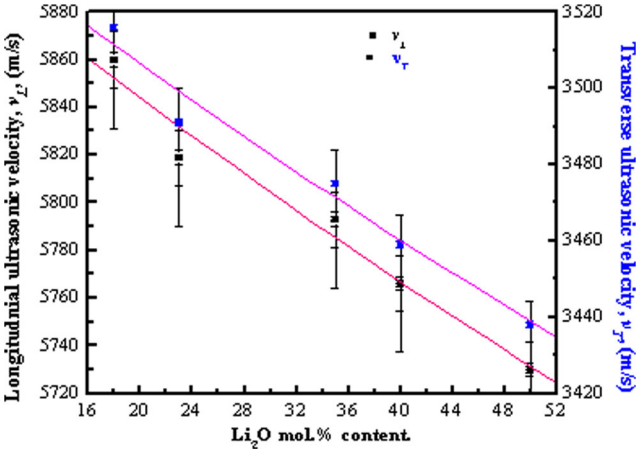

Fig. 8 Dependence of the longitudinal and shear ultrasonic velocities vL and vT of the investigated glasses

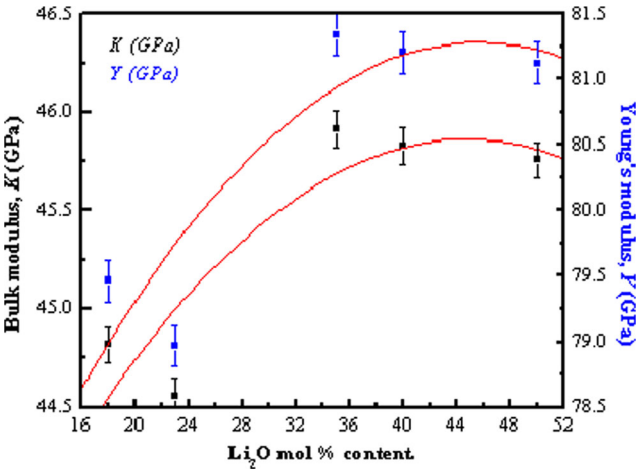

Fig. 9 Composition dependence of the Young's modulus (Y) and bulk modulus (K) of the studied glasses

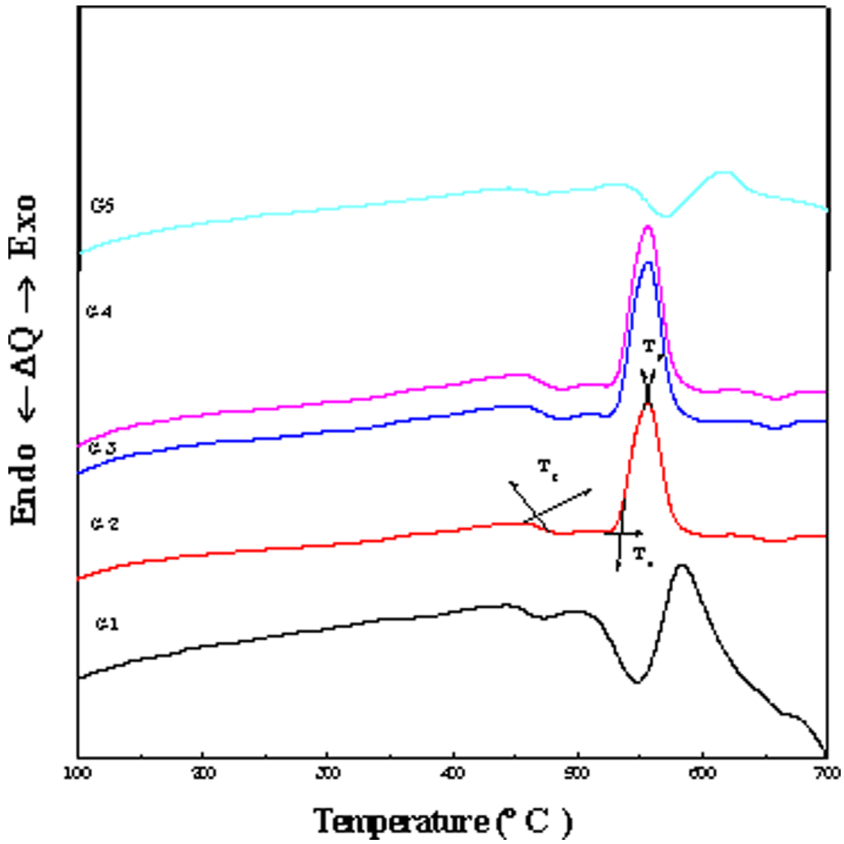

Fig. 10 DTA curve of the studied glasses

the decrease in the average force constant and to the bond strength as suggested from the analysis of the behavior of the ultrasonic velocities. The two parameters indicated a decrease in the rigidity of the glasses as the Li_2O content increases.

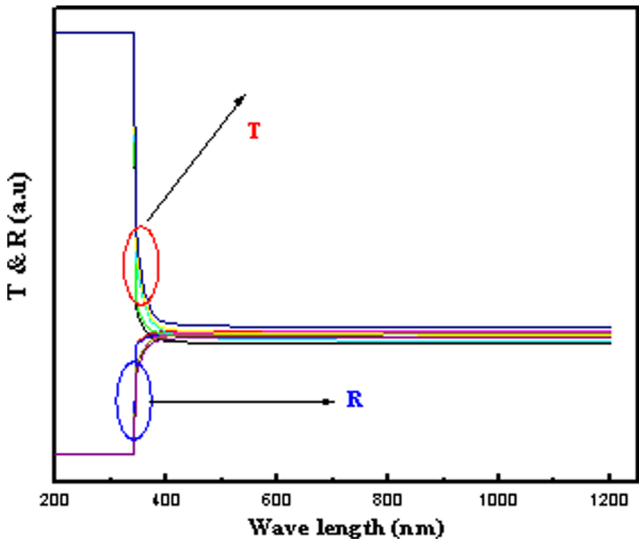

Fig. 11 Transmittance and reflectance (T&R) spectra for the studied glasses

The thermal stability criterion ΔT is a rough measure of the glass thermal stability so larger differences between T_c and T_g indicate more stable glasses. Higher values of H_g and *S* reflect greater thermal stability of the glass. It is found that the ΔT, Hg and S values increase as listed in Table 4 with increasing Li_2O content, i.e., the glass thermal stability increases with increasing Li_2O content.

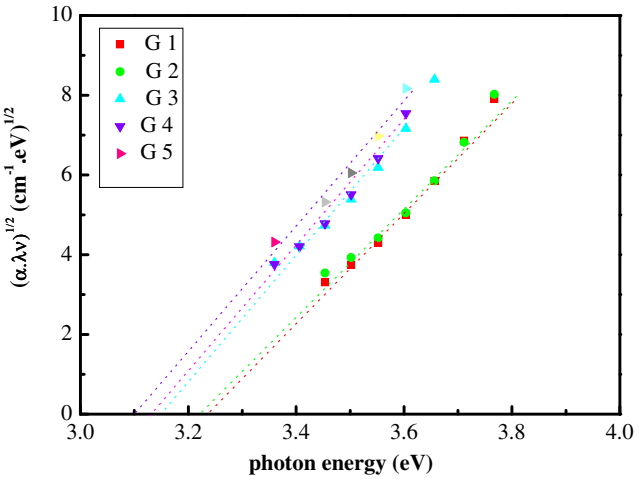

Fig. 12 Plot of $(\alpha\ h\nu)^{1/2}$ against photon energy (eV)

Table 4 Thermal parameter values

Glass number	T g (°C)	Tc (°C)	Tp (°C)	Δ T (°C)	Hg	S	E_g (eV)
G1	507	563	584	56	0.11	2.32	3.25
G2	469	535	556	66	0.141	2.955	3.225
G3	467	530	555	63	0.135	3.373	3.15
G4	466	533	554	67	0.144	3.019	3.125
G5	460	586	615	126	0.274	7.943	3.1

3.4 UV Absorption Spectra

The UV-Vis-NIR absorption spectra are a useful method for optical investigation of induced transitions and providing information about the band structure and energy gap of the glasses [24]. The number of excited electrons into the conduction band, and the electrical and optical properties are a function of both the temperature and the energy band gap E_g.

Figure 11 depicts the measured transmittance and reflectance (*T&R*) spectra for the studied glasses. It is found that the optical absorption edge is not sharply defined in the present glasses, which clearly indicates their glassy nature. As illustrated in this figure, the addition of Li_2O shifts the optical spectra to the high wavelength side (i.e. to the red-shift of the optical band gap) [25, 26]. This shift is expected as the rigidity of the glasses decreased as the Li_2O increased. The deduced values for E_g are shown in Fig. 12 which represents an insulator material. The values of E_g decrease with the increasing Li_2O content because the width of localized states (γ) increases and also the number of non-bridging oxygens. This means that the excited electrons are less constricted which decreases the optical energy band gap, see Table 4.

According to the Lorentz–Lorenz equation, the density of the material affects the refractive index in direct proportion. Thus, the increase in the values of the refractive index as shown in Fig. 13 is ascribed to the increase of the glass density that was attributed to the variation of the structural units as deduced from FTIR analysis.

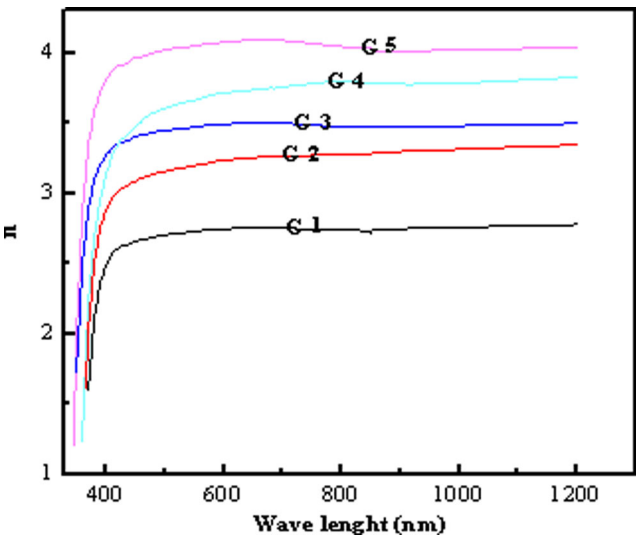

Fig. 13 The refractive index for the studied glasses

4 Conclusion

The physical, structural and optical properties of the studied glass samples depend on the Li_2O content. The increase in the density and consequently the refractive index along with a decrease of the molar volume with Li_2O content were attributed to the formation of dense [BO_4] structural units. The average force constant and the bond strength of Li–O are lower than B–O, so the rigidity of the glasses is reduced. This reduction decreases the T_g, the ultrasonic velocity and the optical energy band gap. The parameters of the thermal stability ΔT, Hg and S values increase with increasing Li_2O content.

References

1. Reddy MS, Raju GN, Nagarjuna G, Veeraiah N (2007) J Alloys Comput 438:41–51
2. Halima MK, Chiew WH, Sidek HAA, Daud WM, Wahab ZA, Khamirul AM, Iskandar SM (2014) Sains Malays 43(6):899–902
3. Rao LS (2009) J Solid State Sci 11:578–587
4. Kafhief I, Rahman SA, Mostafa AG, Ibrahim EM, Sanad AM (2008) J Alloys Compd 352:450
5. Doweidar H, El-Damrawi G, Al-Zaibani M (2013) J Vib Spectrosc 68:91–95
6. Hwa L, Hwang S, Liu L (1998) J Non-Cryst Solids 238:193
7. Abd-El Ghany AM (2015) Spectrosc Lett 48:623
8. Abdelghany AM, Zeyada HM, ElBatal HA, Fetouh R (2010) Silicon 2(3):179
9. Saddeek Y, Abousehly A, Hussien S (2007) J Phys D Appl Phys 40:4674
10. Gowda V, Reddy C, Radha K, Anavekar R, Etourneau J, Rao K (2007) J Non-Cryst Solids 353:1150

11. Baccaro S, Monika, Sharma G, Thind KS, Singh D, Cecillia A (2007) J Nucl Instrum Methods B 260:613
12. Kamitsos EI, Ptsis AP, Karakassides MA, Chryssikos GD (1990) J Non-Cryst Solids 126:52
13. Cheng Y, Xiao H, Guo W (2007) J Ceram Int 33:1341
14. Kamitsos E, Karakassides M, Chryssikos G (1987) J Phys 91: 1073
15. Rao LS (2009) J Solid State Sci 11:578–587
16. Doweidar H (1990) J Mater Sci 25:253
17. Cottrell TL (1958) The strengths of chemical bonds, 2nd edn. Butterworth, London
18. Darwent BdeB (1970) National Standard Reference Data Series, National Bureau of Standards, no. 31, Washington
19. Benson SW (1965) J Chem Educ 42:502
20. Kerr JA (1966) Chem Rev 66:465
21. Saddeek YB, Aly KA, Bashier SA (2010) Phys B Condens Matter 405:2407–2412
22. Saad M, Poulain M (1987) J Mater Sci Forum 19:11–18
23. Wang JS, Vogel EM, Snitzer E (1994) J Opt Mater 3:187
24. Wang JS, Vogel EM, Snitzer E (1994) J Opt Mater 3:187
25. Aly KA (2009) J Non-Cryst Solids 355:1489–1495
26. Aly KA, Abousehly AM, Osman MA, Othman AA (2008) J Phys B Cond Matter 403:1848–1853